HHS Public Access

Author manuscript

ACS Nano. Author manuscript; available in PMC 2021 November 24.

Published in final edited form as:

ACS Nano. 2020 November 24; 14(11): 15083–15093. doi:10.1021/acsnano.0c05091.

Multivalent, Soluble Nano-Self Peptides Increase Phagocytosis of Antibody-Opsonized Targets while Suppressing "Self" Signaling

AbdelAziz R. Jalil,
Biophysical Engineering Laboratories and Department of Chemistry, University of Pennsylvania, Philadelphia, Pennsylvania 19104, United States;

Brandon H. Hayes,
Biophysical Engineering Laboratories and Bioengineering Graduate Group, University of Pennsylvania, Philadelphia, Pennsylvania 19104, United States

Jason C. Andrechak,
Biophysical Engineering Laboratories and Bioengineering Graduate Group, University of Pennsylvania, Philadelphia, Pennsylvania 19104, United States;

Yuntao Xia,
Biophysical Engineering Laboratories, University of Pennsylvania, Philadelphia, Pennsylvania 19104, United States

David M. Chenoweth,
Department of Chemistry, University of Pennsylvania, Philadelphia, Pennsylvania 19104, United States;

Dennis E. Discher
Biophysical Engineering Laboratories and Bioengineering Graduate Group, University of Pennsylvania, Philadelphia, Pennsylvania 19104, United States;

Abstract

Macrophages engulf "foreign" cells and particles, but phagocytosis of healthy cells and cancer cells is inhibited by expression of the ubiquitous membrane protein CD47 which binds SIRPα on macrophages to signal "self". Motivated by some clinical efficacy of anti-CD47 against

Corresponding Author: Dennis E. Discher – Biophysical Engineering Laboratories and Bioengineering Graduate Group, University of Pennsylvania, Philadelphia, Pennsylvania 19104, United States; discher@seas.upenn.edu.

Author Contributions

A.R.J. and D.E.D. designed the research, prepared the figures, and wrote the manuscript. A.R.J. performed all in vitro experiments. B.H.H. assisted with phagocytosis assays, data analysis, flow cytometry, gene expression analysis, and manuscript revisions. J.C.A. performed the *in vivo* experiments, mouse blood parameter analyses, and manuscript revisions. Y.X. performed confocal microscopy. D.M.C. provided laboratory space, is a co-adviser on the research project, and assisted in reviewing the manuscript.

Supporting Information

The Supporting Information is available free of charge at https://pubs.acs.org/doi/10.1021/acsnano.0c05091.

Analytical HPLC and chromatograms, MALDI-TOF spectra, microarray gene expression analysis, opsonin titration curves, mouse macrophage phagocytosis assay, flow cytometry, binding assays, circular dichroism, and infrared spectra (PDF)

Complete contact information is available at: https://pubs.acs.org/10.1021/acsnano.0c05091

The authors declare the following competing financial interest(s): A.R.J. and D.E.D. declare submission of a U.S. patent application, Multivalent Nano-Self Peptides and Uses Thereof.

liquid tumors and based on past studies of CD47-derived polypeptides on particles that inhibited phagocytosis of the particles, here we design soluble, multivalent peptides to bind and block SIRPα. Bivalent and tetravalent nano-Self peptides prove more potent (K_{eff} ~ 10 nM) than monovalent 8-mers as agonists for phagocytosis of antibody opsonized cells, including cancer cells. Multivalent peptides also outcompete soluble CD47 binding to human macrophages, consistent with SIRPα binding, and the peptides suppress phosphotyrosine in macrophages, consistent with inhibition of SIRPα's "self" signaling. Peptides exhibit minimal folding, but functionality suggests an induced fit into SIRPα's binding pocket. Pre-clinical studies in mice indicate safety, with no anemia that typifies clinical infusions of anti-CD47. Multivalent nano-Self peptides thus constitute an alternative approach to promoting phagocytosis of "self", including cancer cells targeted clinically.

Graphical Abstract

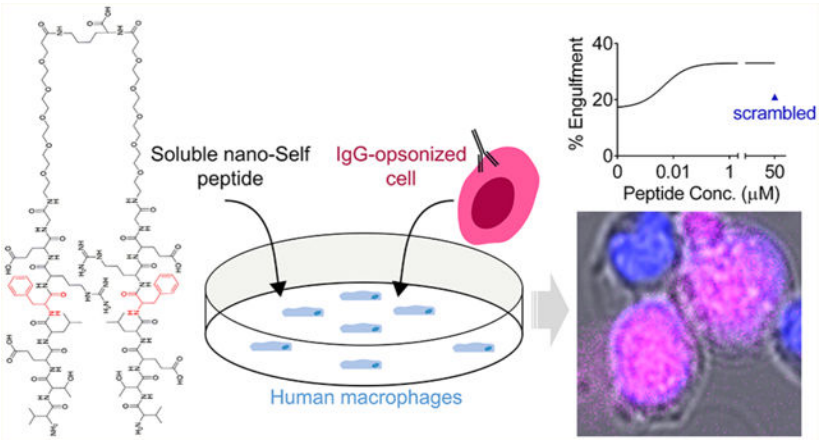

Keywords

peptide; macrophage; immune blockade; antibody; CD47; signal regulatory protein-α

Protein-mediated interactions between two cells can convey inhibitory signals such as with the various "checkpoint" receptors on immune cells. On macrophages, for example, signal regulatory protein-α (SIRPα) is a checkpoint receptor that binds the ubiquitously expressed protein CD47,[1–4] and the SIRPα-CD47 interaction initiates a signal cascade which inhibits macrophage engulfment of cells or particles that display both CD47 and a macrophage-activating antibody. On T-cells, in comparison, the PD-1 checkpoint receptor binds to PD-L1 displayed on the surface of other cell types,[5,6] and the interaction ultimately inhibits T-cell activation. Importantly, antibody antagonists of these inhibitory, checkpoint interactions enable the respective immune cells to eliminate target cells, particularly cancer cells. However, efficacy is lacking in many cancer patients infused with blocking antibodies,[7–11] and such limitations motivate additional molecular designs.

Nearly half of CD47's contact surface with SIRPα localizes to eight residues in a β-hairpin loop within CD47's immunoglobulin (Ig) domain (Figure 1A).[4,12] A 21 amino acid peptide derived from CD47 binds SIRPα and mimics the function of the Ig domain

by inhibiting macrophage-mediated clearance of peptides, or Ig, displaying nanoparticles injected in mice.[12] Mechanistically, CD47 stimulates SIRPα phosphorylation to signal against phagocytosis.[13–18] The CD47-SIRPα macrophage checkpoint is already targeted in cancer patients with antagonizing antibodies and with antibody-like bivalent fusions of SIRPα.[19–23] Although blockade can be effective in some patients with liquid tumors when combined with a tumor-opsonizing IgG,[24] infusion of anti-CD47 is often seen to clear blood cells including red blood cells (RBCs).[25–27] We hypothesized that a multivalent, eight amino acid nano-Self (nS) peptide could antagonize SIRPα while preventing the clearance of blood cells *in vivo*. Here, multivalent peptides substituted at a single key residue (Figure 1B) function as SIRPα antagonists and lead to an increased phagocytosis of antibody-targeted cells as well as association with and net dephosphorylation within macrophages. Compared to large antibodies, the much smaller nS peptides potentially represent an additional class of macrophage checkpoint inhibitors.

RESULTS AND DISCUSSION

Nano-Self Peptide Designs, Synthesis, and Characterization.

CD47's eight amino acid binding loop defines a wild-type nano-Self (nS-wt) and has a central Thr next to a hydrophobic Leu that are both buried in SIRPα's hydrophobic pocket (Figure 1A). All co-crystal structures of CD47 and its antagonists show an interaction with this central Thr.[28] Furthermore, screening for high affinity mutants of SIRPα's binding pocket all yielded Phe insertions (with >100-fold higher affinities for CD47 *versus* the sub-μM affinity of wild-type),[20] which suggests that a greater hydrophobicity and/or aromaticity increases affinity. We therefore substituted the Thr with hydrophobic Phe or Val (nS-F and nS-V, respectively, in Figure 1B, inset table). Phe adds aromaticity and could allow for a π-stacking interaction with SIRPα's Phe-74 that points towards CD47's key β-hairpin, whereas Val removes the polar hydroxyl group from the similarly sized Thr. Multivalent nS peptide designs are motivated in part by the fact that SIRPα is mobile—it accumulates at the phagocytic synapse[15] and is likely a homodimer.[29] A distance of ~2.5 nm between the binding sites of SIRPα homodimers was estimated from simple modeling of crystal structures and led us to design bivalent nS peptides with two flexible PEG_5 nano-linkers of ~1.5 nm length[30] attached to two amines of a bridging Lys (Figure 1B).

All nS peptides were synthesized on a Rink amide resin yielding C-terminal amide functional groups to minimize the charge on the peptides. Analytical HPLC followed by matrix-assisted laser desorption ionization-time of flight (MALDI-TOF) mass spectrometry characterization showed >98% purity of all synthesized nS peptides (Figure S1). Solubility at neutral pH (up to at least 50 μM) is likely attributable to charge on three of the eight residues.

nS Peptide Agonists for Human Macrophage Engulfment of Opsonized Human Cells.

Solutions of nS peptides were added to cultures of adherent human THP-1 macrophages (referred to as macrophages; Figures 2A and S2) to study the phagocytosis of two antibody-opsonized human cells: (1) healthy RBCs which serve as a simple "self" cell and are also relevant to the anemia caused by anti-CD47 infusion; and (2) human erythroleukemia

K562 cells which serve as a blood cancer cell model relevant to the liquid tumors that show some efficacy when treated with opsonized IgG and anti-CD47.[24] After observing and quantifying internalization of RBCs with our bivalent nS-FF peptide by macrophages, we further synthesized a tetravalent peptide to study the effects of multivalency on cancer cells (Figures 2B and S3). Interestingly, all nS peptides, except for scrambled nS-X and nS-XX, enhanced the phagocytosis of RBCs opsonized by anti-RBC IgG (Figures 2C and S4). nS-FF was effective even at 20 nM with ~40% of peptide-treated macrophages showing at least one opsonized RBC internalized by the end of the 1 h assay, with an efficacy constant (K_{eff}) of ~8 nM, indicating a >100-fold higher activity than that of nS-wt (Figure 2C). This key metric of efficacy in promoting phagocytosis follows the trend: nS-FF > nS-F > nS-VV > nS-V > nS-wt > nS-X = 0 activity (Figure 2C).

Furthermore, maximum peptide concentrations of 50 μM show phagocytosis levels for nS-wt and all nS-F and nS-V variants are well above those for nS-X and nS-XX controls that do not affect baseline engulfment of opsonized RBCs (Figure 2C,D).

Maximum peptide concentrations reveal an additional effect when compared to anti-CD47 on the RBC. Combining anti-CD47 with anti-RBC causes ~30% of macrophages to phagocytose the opsonized RBCs, which is higher than the effect of anti-RBC alone (~20% of macrophages contain opsonized RBCs; red open bar in Figure 2D). The result is consistent with anti-CD47 inhibiting recognition by the macrophage's SIRPα. Likewise, combining nS-wt with anti-RBC also causes ~30% of the macrophages to internalize opsonized RBCs. Note that saturating amounts of anti-CD47 on RBCs has a minimal effect on baseline engulfment (~5–10% of macrophages) and that anti-RBC is always used at ~133 nM (Figure S5A). Surprisingly, the highest levels of phagocytosis, with ~40–50% of macrophages containing opsonized RBCs, are seen for all F and V substituted peptides at maximum peptide concentrations (Figure 2D).

Opsonized erythroleukemia K562 cancer cells were similarly tested for phagocytosis in the presence of our most potent nS-FF and our tetravalent nS-F4 peptides. The anti-RBC successfully opsonized and triggered phagocytosis of K562 cells by macrophages (Figures 2E,F and S5B). Multivalent nS-FF and nS-F4 nearly doubled the percentage of phagocytic macrophages relative to *trans* anti-CD47 blockade, whereas macrophages were unaffected by nS-XX control (Figure 2F). Interaction of the nS peptides with K562 cells is likely minimal due to the relative lack of SIRPα expression (Figure S2). However, saturation at ~40% of macrophages engulfing opsonized K562 cells is less than the ~50% for opsonized RBCs, perhaps because K562 cells have more CD47 molecules than RBCs, suggesting more "don't eat me" signaling (Figure S6).

For both opsonized RBCs and opsonized K562s (Figure 2D,F), the hyper-phagocytosis that is achieved with soluble F- and V-nS peptides matches the recently measured increases for disruption of both the *trans* interactions between CD47 on a target and macrophage SIRPα and also, importantly, the *cis* interactions between CD47 and SIRPα on the same macrophage (Figure 2G, left).[31] Expression profiling of macrophages confirms these cells generally express CD47 at similar levels to other cell types (Figure S2). The recent study of the *cis* interaction showed that a macrophage-CD47 knockdown removed a basal level of

inhibitory “self” signaling from the *cis* interaction and thereby caused hyper-phagocytosis, with similarly increased phagocytosis when anti-CD47 was added to macrophages separate from adding anti-CD47 to the targeted RBC. A preliminary conclusion is that nS-FF and the other substituted peptides, which were designed to bind SIRPα, inhibit both the *cis* and *trans* interactions between SIRPα and CD47 (Figure 2G, right).

Consistent with the results with human macrophages, mouse-derived J774A.1 macrophages show all of the same trends for nS-F, nS-V, nS-wt, and nS-X peptides, including 3-fold more phagocytosis with nS-F relative to the minimal internalization of opsonized RBCs in the presence of nS-X control (Figure S5C). The ~10–20% increase in phagocytic mouse macrophages with F- and V-substituted nS peptides relative to anti-CD47 on opsonized RBCs agrees with the *cis* and *trans* inhibition effect, and the nS-wt peptide matches anti-CD47 blockade effects, at least for high concentrations (50 μM). Indeed, the effective activity of nS-wt is ~100-fold weaker in the mouse macrophage assay than in the human assay (Figure 2C). The difference could reflect a singular difference between the eight residue sequences of human and mouse CD47’s: The Thr in human-CD47 is replaced by a less bulky and less hydrophobic Ser in mouse-CD47, which again affirms that sequence matters. The various phagocytosis results lead us to further hypotheses on peptide functions (Figure 2G). First, the nS-F peptide should associate directly with macrophages, and moreso than nS-X but less so than nS-FF. Second, nS-F and nS-FF peptides affect phosphotyrosine levels that are downstream of SIRPα binding to CD47.[31]

Multivalent nS Peptides inhibit CD47-Fc Binding to Human Macrophages.

To determine whether the nS peptides bind to SIRPα, we used nS-FF and nS-F4 as soluble competitive inhibitors of saturable CD47-Fc fusion protein binding to macrophages (Figure S7). An addition of multivalent nS peptides was followed by a Fc-receptor blockade to minimize the Fc-driven binding of constructs. Afterwards, CD47-Fc was added prior to anti-Fc fluorescence imaging (Figure 3A). Quantitation of fluorescence shows the expected trend for the levels of inhibition:

$$\text{nS-F4}\sim\text{nS-FF} > \text{nS-wt} > \text{nS-XX} \ (=0)$$

Anti-CD47 was pre-incubated with CD47 as a positive control for the inhibition of binding to SIRPα.[28] This showed that both nS-F4 and nS-FF are as inhibitory as anti-CD47.

Tyrosine Phosphorylation in Macrophages Is Suppressed by nS Peptides.

Given that the interaction of CD47 with SIRPα initiates a de-phosphorylation cascade regardless of whether the interaction occurs in *trans* or in *cis*,[15,31] two key nS peptides were again added to the macrophages for quantitative fluorescence microscopy. Basal levels of phosphotyrosine (pTyr) in wild-type macrophages are indeed suppressed by nS-FF and by anti-CD47 (Figure 3B). Importantly, nS-FF suppressed the pTyr signal at the low peptide concentration (20 nM; Figure 3B), that maximizes phagocytosis by blocking both *trans* and *cis* interactions (Figure 2C). Monovalent nS-F at the high concentration (50 μM), which likewise maximized phagocytosis, also suppressed pTyr, whereas 20 nM nS-F did not significantly affect pTyr, consistent with blocking only *trans* interactions at the low

concentration (Figures 2C,D). The negative control peptide nS-X (50 μM) had no effect on pTyr, which is consistent with the lack of effect in phagocytosis. Note that anti-CD47 in the phagocytosis studies was added to the opsonized RBCs and K562 cells blocking only the *trans* interactions, whereas in these pTyr experiments (Figure 3B), anti-CD47 was added to the macrophages to determine the effect on basal signaling in the absence of phagocytosis. The pTyr results are not only consistent with peptide disruption of *cis* interactions between CD47 on the surface of the macrophage and SIRPα (Figure 3C) but also further underscore the functional potency of multivalent nS peptides.

Competitive Binding of nS peptides to Macrophages.

To assess peptide association, nS-F was fluorescently labeled (denoted nS-F-fluor) and added to macrophages. Fluorescence microscopy shows nS-F-fluor associates with all cells (Figure S8A, Ctrl), consistent with SIRPα expression on all macrophages. Some evidence of internalized fluorescent peptide signal is consistent with SIRPα internalization as part of the recycling of such cell surface receptors.[32–34] To demonstrate the increased affinity of bivalent nS peptides relative to monovalent nS-F, unlabeled nS-FF and nS-VV were added as inhibitors to cultures with 100 μM nS-F-fluor. Bivalent peptides at just 20 nM significantly decreased association of nS-F-fluor with macrophages, whereas nS-X showed no effect up to 50 μM (Figure S8B).

Biotinylated-nS peptides were also used to confirm association with SIRPα by incubating streptavidin-coated polystyrene micro-beads first with a biotinylated nS and then with purified recombinant human SIRPα extracellular domain[15] plus fluorescent (non-blocking) anti-SIRPα (Figure S9). Given the effect on phagocytosis after the addition of nS peptides to both human and mouse macrophages, association of nS-fluor peptides with both species of macrophages was investigated. From imaging analysis, there was indication of internalization similar to the anti-mouse SIRPα (P84-FITC) (Figure S10A,B), especially at high peptide concentrations ($\gg$1 μM). For nS-X which showed no effect on phagocytosis, total fluorescence intensity of nS-X-fluor associating with the macrophages proved significantly lower and >5-fold weaker than the other functional peptides (Figure S10C).

nS Peptides Are Mainly Disordered, with Binding Likely to Enhance β-Hairpin Structure.

Because of the snug fit of the key CD47 β-hairpin within SIRPα (Figure 1A), we investigated the secondary structures of the eight amino acid peptides in solution, using circular dichroism (CD) (Figures 4 and S11). At low temperatures (5 °C), the peptides are largely random coils with a minor fraction of β-turn structure when compared to other short peptides.[35–37] This is evident for the most functional peptide nS-FF as a slight positive ellipticity peak at 215–220 nm and deep negative ellipticity peak around 195 nm — signals that are somewhat clear for the slightly less functional nS-VV peptide but much attenuated for nS-XX or nS-X. Thermal unfolding at 90 °C is evident in the suppression of the ellipticity peaks. Difference spectra (Figure 4B) are the same for the bivalent nS-FF and nS-VV, whereas nS-XX is attenuated, showing a trend similar to the phagocytosis results (Figures 2C–F).

The nS peptides here are mainly random coils (Figures 4A and S11), which suggests an induced fit association with SIRPα on macrophages. Phagocytosis levels of nS peptide-treated macrophages were compared to the anti-CD47 blockade of the target, with bivalent nS-FF and tetravalent nS-F4 proving to be more potent in enhancing phagocytosis at pharmacologically relevant concentrations (20 nM) (Figures 2C–F). The slight increase of phagocytic macrophages when cultured with nS-F4 *versus* nS-FF (Figure 2F) seems consistent with increased avidity as a soluble inhibitor (Figure S12), which supports an advantage of multivalency, even though the effects plateau. The increased levels of target phagocytosis are consistent with *cis* and *trans* inhibition,[31] and nS-FF's suppression of phosphorylation in isolated macrophages is consistent with blocking of the *cis* binding of SIRPα to CD47 (Figure 3B,C).

Safety of ns-FF Injections in a Pre-Clinical Test.

Phase 1 clinical trials for safety of anti-CD47 in patients have shown that infusion into the bloodstream decreases RBC numbers (*i.e.*, hematocrit) and increases reticulocytes (*i.e.*, new RBCs),[19,26] and related blood safety concerns apply to a bivalent CD47-binding protein made with SIRPα domains fused to a macrophage-binding Fc domain.[38] Given that our nS-F peptide increases phagocytosis of opsonized RBCs and also associates with mouse macrophages (Figures S5 and S10), we assessed the safety of the more potent nS-FF peptide by intravenous injection into mice. Overall, nS-FF in PBS showed no differences *versus* the PBS vehicle control in its effects on mouse hematology and body weight after four daily tail-vein injections of 1 mg/kg peptide (Figure 4C). This corresponds to about 8 μM in the blood, assuming rapid mixing and no dilution within the ~1.5 mL blood volume of the mouse. Withdrawal of ~140 μL from this blood volume was necessary to obtain a complete hematology profile, and such a volume is expected to cause slight decreases in the hematocrit and platelets as shown in Figure 4C-i,ii. Consistent with this loss, more RBCs should be produced in each mouse to compensate for the RBC loss, and the ~30% increase in reticulocytes after the first two blood draws over 11 days (Figure 4C-iii) is similar to the prior amount of blood removed (~300 μL/1500 μL). The mice (~14 weeks) also continued to gain weight at the same rates (~5% over 11 days) regardless of peptide injections. These changes are thus expected but, importantly, unaffected by the nS-FF peptide. The results establish some initial safety for nS-FF.

CONCLUSIONS

Peptide-based therapies are numerous,[39] and for cancer, they include approved analogs of naturally occurring molecules (*e.g.*, bortezomib, carfilzomib, and goserelin). In cell adhesion signaling, for example, the tripeptide RGD that was derived from proteins in extracellular matrix[40] led to a synthetic analog with increased affinity for matrix receptors[41] and with utility as a soluble competitive inhibitor of adhesion in clinical trials against cancer.[42] Peptides are usually synthesized at low cost (~$1/mg in the United States) and can be stored at a high concentration relative to therapeutic IgG's.[43] To be clear, lab-grade anti-CD47, anti-SIRPα, and anti-PD1 are ~$100/mg, and clinical-grade antibodies such as anti-PD1 cost >$100,000/patient/year.[44,45] Moreover, very few residues in a ~150 kDa antibody physically contact a target antigen.

The 21 amino acid “Self” peptide was the first peptide shown to bind SIRPα and recapitulate the anti-phagocytic signaling of full-length CD47. Although a similar 21 amino acid peptide was modified for surface immobilization and reported to not bind soluble SIRPα,[46] our eight amino acid nano-Self peptides show clear and consistent functionality. First, they enhanced phagocytosis of IgG-opsonized human cells (normal and cancer) by human macrophages, and secondly the peptides were as effective as anti-CD47 in inhibiting a CD47-Fc construct in binding to human macrophages. Anti-CD47 infusions in the clinic cause anemia,[24] that could in part reflect the Fc function of anti-CD47 because anemia is not evident with initial infusions of nS peptides.

When displayed on particles, the 21 amino acid “Self” peptide inhibited phagocytosis of IgG opsonized particles,[12] whereas the soluble peptides here function as antagonists. This finding is consistent with the prior use of large, soluble CD47 ectodomains as inhibitors of SIRPα to enhance phagocytosis of tumor cells.[47,48] The smaller peptides here are more likely to penetrate a solid tumor, or they might be delivered to tumors (which are typically rich in macrophages) by various methods that range from nanoparticle-mediated “nano-gene” therapy to packaging them into peptide-secreting bacteria[49] or perhaps backpacks that attach to tumor-injected macrophages.[50] In contrast to nS peptides, anti-CD47 can in principle directly opsonize healthy or diseased cells and activate engulfment by macrophages; this is because the antibody’s Fc-domain activates the Fc receptor on the macrophages.[51,52] On the other hand, such an effect is not evident in our data with the B6H12 clone of anti-CD47.[15] Regardless, a bivalent anti-CD47 nanobody that lacks an Fc domain caused modest anemia and mild thrombocytopenia in mice (following a similar injection and bleeding protocol as used here), and addition of an Fc domain to the nanobody increased these adverse effects.[53] Once again, the nS peptides lack an activating Fc domain and should solely antagonize SIRPα, eliminating opsonization, and thereby minimizing clearance of healthy cells.

In summary, synthesis and functional tests of multivalent, CD47-inspired nano-Self peptides with hydrophobic substitutions at a central Thr demonstrate potential as a nanomolar agonist for phagocytosis of targeted diseased cells such as cancer cells. Sequence analyses of various species beyond human and mouse[28] suggest the nS peptides will function with macrophages in monkeys and dogs, which are important species for evaluation of safety and efficacy. Lastly, the increased phagocytosis of soluble nano-Self relative to anti-CD47 on the cell that is targeted for phagocytosis certainly motivates further investigation of CD47-SIRPα’s molecular mechanisms.

EXPERIMENTAL METHODS

Solid-Phase Peptide Synthesis.

Standard Peptide Synthesis.—All peptides in this study were synthesized on a Rink Amide MBHA Resin (loading density: 0.33 mmol/g; Novabiochem) on a 100 μmol scale at room temperature (RT) using 9-fluorenylmethoxycarbonyl (Fmoc) chemistry. The resin was transferred to a solid-phase peptide synthesis vessel and swelled in *N,N*-dimethylformamide (DMF; Sigma) for 30 min with stirring. Deprotection of the Fmoc group was achieved by using 1 mL of 1% w/v 1-hydroxybenzotriazole (EMD Millipore) and 2% v/v 1,8-

diazabicyclo[5.4.0]undec-7-ene (Acros Organics) in DMF and left to stir for 1 min (repeated three times). Lastly, the resin was then washed thoroughly with DMF. Coupling solutions contained 3 equiv of Fmoc-amino acids (Chem-Impex or Oakwood Chemicals), 2.8 equiv of 1-[bis(dimethylamino)-methylene]-1H-1,2,3-triazolo[4,5-*b*]pyridinium 3-oxid hexafluorophosphate (HATU; Oakwood Chemicals), and 6 equiv of *N,N*-diisopropylethylamine (DIEA; Sigma) – relative to resin – dissolved in a minimal amount of DMF to cover the resin (1–1.3 mL) and were activated for 5 min at RT prior to addition to resin. Coupling reactions were left to proceed for 1 h. Following each coupling reaction, the resin was drained, washed thoroughly with DMF, deprotected as described above, and washed thoroughly with DMF.

Bivalent Peptide Synthesis.—Bivalent peptides were prepared by coupling 3 equiv of Fmoc-Lys(Fmoc)-OH directly on the resin and deprotecting the Fmoc groups following the same procedure mentioned above. The coupling solutions of the polyethylene glycol (PEG) acids contained 5 equiv of Fmoc-NH-PEG_5-CH_2CH_2COOH (PurePEG), 4.5 equiv of HATU, and 10 equiv of DIEA. The coupling reactions were left to proceed for 3 h. Every subsequent amino acid coupling was done using 6 equiv of Fmoc-amino acid, 5 equiv of HATU, and 10 equiv of DIEA.

5(6)-Carboxyfluorescein Coupling.—All fluorescently labeled peptides were prepared by coupling Boc-Lys(Fmoc)-OH at the N-terminus and deprotection of the Fmoc-protected γ-amine of Lys. 5(6)-Carboxyfluorescein (FAM) (Chem-Impex) was prepared by dissolving 2 equiv in DMF with 2 equiv of HATU and added to the resin after activation for 5 min at RT. In order to maintain a homogenous solution, 6 equiv of DIEA was added dropwise to the stirring solution.[54] The reaction was left to proceed overnight in the dark.

Peptide Cleavage.—Following the final deprotection of the last Fmoc group (except for fluorescent peptides where the last amino acid contains an acid labile Boc protecting group), the resin was washed with DMF twice and then twice more with dichloromethane (DCM; Sigma). A 5 mL cleavage cocktail containing 95% trifluoracetic acid (TFA; Acros Organics), 2.5% H_2O, and 2.5% triisopropylsilane (TIPS; Oakwood) was added to the reaction vessel and left to stir for 4 h. 45 mL of cold diethyl ether (Sigma) was then added to the cleavage solution precipitating the peptide. To make sure all of the peptide precipitated, the ether layer was evaporated by air until ~10 mL of solution was left; thereafter, an additional 40 mL of cold ether was added. The peptide was collected by centrifugation, resuspended in cold ether, and collected by centrifugation again (repeated three times). Depending on the solubility of the peptide, the ether washed pellet was dissolved in a mixture of 10–40% acetonitrile (ACN; Sigma) in water.

Purification and Characterization.—All peptides were purified using preparative reversed-phase high-performance liquid chromatography (HPLC) on an Agilent 1260 Infinity II system using a Phenomenex Luna Omega 5 μm PS C18 100 Å LC column. Varying gradients of ACN and 0.1% TFA in H_2O were used to separate the respective peptides. Purity of each peptide was checked using an analytical Agilent 1260 Infinity II system using a Phenomenex Luna Omega 5 μm PS C18 100 Å LC column. Mass

spectrometry was performed using a Bruker matrix-assisted laser desorption ionization–time of flight (MALDI-TOF) Ultraflex III mass spectrometer and α-cyano-4-hydroxycinnamic acid (CHCA; Sigma) as the matrix. Peptides were lyophilized using a Labconco FreeZone Plus 12 Liter Cascade Console Freeze Dry system.

UV–vis, Circular Dichroism, and Fourier Transform Infrared Measurements.—UV–vis absorption spectrophotometry was performed using a Jasco V-650 spectrophotometer and 1 cm path length quartz cells. Lyophilized peptide was dissolved in 100 μL of phosphate buffered saline pH 7.4 (PBS; Thermo Fischer), and the concentration of each peptide was determined by measuring the absorbance at 205 nm and using a calculated extinction coefficient for each peptide due to the lack of aromatic residues in the peptides.[55,56] For fluorescein-labeled peptides, the lyophilized solid was dissolved in 20 μL of dimethyl sulfoxide (Sigma) and then diluted to 100 μL with PBS. Peptide concentration was determined by measuring the absorbance at 495 nm.

Circular dichroism (CD) experiments were performed using a Jasco J-1500 circular dichroism spectrometer and 1 mm quartz cuvettes. 100 μM samples were prepared for each peptide in sodium phosphate buffer pH 7, and ellipticity was measured from 190 to 260 nm at 5 °C and 95 °C, respectively.

Fourier transform infrared (FT-IR) measurements were collected using a Jasco FT/IR-6800 FT-IR spectrometer. Peptide samples were solvent swapped into deuterated water and deuterated hydrochloric acid. 5 μL droplets of peptide samples were measured at RT, and the absorbance was recorded from 1200–1700 cm^{-1}.

Cell Culture.

All cells were purchased from American Type Culture Collection (ATCC). Human derived THP-1 monocytes and mouse J774A.1 macrophages were both cultured in RPMI 1640 media (Gibco). Human erythroleukemia K562 cells were cultured in IMDM media (Gibco). All media were supplemented with 10% v/v fetal bovine serum (FBS; Sigma) and 1% v/v penicillin/streptomycin (Sigma). J774A.1 macrophages were grown either as suspension or adherent cultures. To passage adherent J774A.1 macrophages, the cells were gently scraped with a cell scraper (Corning). THP-1 monocytes were cultured in suspension. Differentiation of THP-1 monocytes to macrophages was achieved by the addition of 100 ng/mL of phorbol myristate acetate (PMA; Sigma) in media for 2 days (unless stated otherwise) and confirmed by attachment of the macrophages to the bottom of the tissue culture plates.

In Vitro Phagocytosis Assay.

Fresh human RBCs were washed twice with 50 mM EDTA (Thermo Fischer) in Dulbecco's phosphate buffered saline (PBS; Gibco) and then twice with 5% FBS in PBS. RBCs were opsonized with 20 μg/mL rabbit anti-human RBC IgG (Rockland) in 5% FBS for 1 h at RT with shaking. For CD47 blocked RBCs, 5 μg/mL of mouse anti-human CD47 (B6H12; BD Biosciences) was added. Thereafter, RBCs were washed with PBS three times and stained with PKH26 dye (1:800 dilution in PBS; Sigma) for 1 h at RT with shaking in the dark. RBCs were washed and resuspended in PBS.

THP-1 monocytes were PMA differentiated in RPMI for 48 h. Macrophages were then washed with RPMI media three times. The macrophages were then incubated with 20 nM, 1 μM, or 50 μM of the nano-Self peptides for 1 h at 37 °C, 5% CO_2, and 95% humidity. The THP-1s were then washed with RPMI three times. J774A.1 macrophages were plated for 24 h in RPMI. The same peptide blocking procedure as above was used with the addition of a positive control using 5 μg/mL rat anti-mouse SIRPα (P84; BD Biosciences).

IgG opsonized RBCs were added to macrophages at a ratio of 10:1 for 1 h at 37 °C, 5% CO_2, and 95% humidity. Macrophages were then washed with RPMI three times. Adherent and uninternalized RBCs were lysed with water for 30 s followed by immediate replacement with RPMI media. In order to distinguish the remaining adherent RBCs from internalized RBCs, opsonized RBCs were stained with AlexaFluor 647 donkey anti-rabbit (binds to rabbit polyclonal opsonin on RBC; Invitrogen) IgG (1:1000), while un-opsonized, CD47 blocked RBCs were stained with AlexaFluor 647 donkey anti-mouse (binds to mouse monoclonal anti-CD47 on RBCs; Invitrogen) IgG (1:1000) for 30 min. After washing, macrophages were fixed with 4% formaldehyde (Sigma) for 15 min at RT, washed with PBS, stained with 1 μg/mL Hoechst 33342 (Invitrogen), and then washed with PBS again.

K562 cells were washed with PBS then stained with 1:10,000 5(6)-carboxyfluorescein diacetate (CFDA; Invitrogen) in PBS for 15 min at RT in the dark. Cells were washed with PBS to remove excess CFDA dye, and then cells were resuspended in IMDM media. K562 cells were IgG opsonized and CD47 blocked using the same antibody concentrations used in the RBC phagocytosis assay (20 μg/mL anti-RBC and 5 μg/mL anti-CD47) for 1 h on ice in the dark. After washing with IMDM, K562 cells were added to macrophages at a ratio of 5:1 for 2 h at 37 °C, 5% CO_2, and 95% humidity. THP-1 macrophages were stained with Hoechst 33342 for 15 min and then extensively washed prior to the addition of the K562 cells. Afterwards, the macrophages were washed, fixed with 4% formaldehyde, and then washed again.

Fluorescence imaging was performed using an Olympus IX71 with a digital EMCCD camera (Cascade 512B) and a 40×/0.6 NA objective. Confocal imaging was done using a Leica TCS SP8 system with 63×/1.4 NA oil-immersion objective. Quantification was done with ImageJ (NIH). At least 200 cells were analyzed, and experiments were repeated at least three times. Two-tailed student’s t-test was used to determine statistical significance.

CD47-Fc Inhibition Assay.

THP-1 monocytes were PMA differentiated in RPMI for 48 h. The macrophages were washed with RPMI media and then incubated with 1 μM or 50 μM of nano-Self peptides for 1 h at 37 °C, 5% CO_2, and 95% humidity. After washing, the macrophages were incubated with Human Trustain FcX Fc receptor blocking solution (Biolegend) for 10 min at RT and then incubated with 2 μg/mL CD47-Fc fusion protein (ACRO Biosystems) for 1 h at 37 °C, 5% CO_2, and 95% humidity. As a negative control, B6H12 was pre-mixed with CD47-Fc at 4 °C on a rotator for 1 h. The macrophages were then washed and incubated with 0.5 μg/mL goat anti-human IgG Fc DyLight 488 (Thermo Fischer) for 1 h at 37 °C, 5% CO_2, and 95% humidity. Finally, the macrophages were washed, fixed, Hoechst 33342 stained, and imaged as described above.

Peptide Inhibition Assay.

THP-1 monocytes were PMA differentiated in RPMI for 48 h. Macrophages were washed with RPMI three times and then incubated with 1 μM or 20 nM nS-FF or nS-VV for 1 h at 37 °C, 5% CO_2, and 95% humidity. Excess peptide was washed with PBS and then 100 μM of FAM-labeled nS-F was added to the bivalent-peptide blocked macrophages for 1 h as above. As a control, 50 μM of nS-X was used instead of bivalent nS peptides. Excess peptides were washed off with PBS, and cells were fixed with 4% formaldehyde for 15 min at RT, washed with PBS, stained with 1 μg/mL of Hoechst 33342, and then washed with PBS again. Fluorescence imaging was performed as described above, and quantification was done using ImageJ.

SIRPα Staining and Confocal Imaging.

THP-1 monocytes were PMA differentiated in RPMI 1640 for 24 h. J774A.1 cells were plated for 24 h in media. Cells were washed with RPMI prior to addition of fluorescent peptides. The peptides were left to incubate for 1 h at 37 °C, 5% CO_2, and 95% humidity. For fixed cell staining, cells were incubated with 4% formaldehyde for 15 min prior to the addition of fluorescent peptides, whereas for live cell staining, fixation was done after incubation with the FAM-labeled peptides. Nuclei were stained with 1 μg/mL of Hoechst 33342. Cells were then washed with PBS three times before analysis. Fluorescence imaging of fixed cells was done as described above. For live cell (without fixation) confocal imaging, cells were washed with respective media three times after nuclei staining instead of PBS. Confocal imaging was done using a Leica TCS SP8 system with 63×/1.4 NA oil-immersion objective. Quantification was done with ImageJ.

Phosphotyrosine Staining.

THP-1 monocytes were PMA differentiated for 48 h. Macrophages were washed with RPMI three times and then incubated with 50 μM and 20 nM of either nS-F or nS-FF for 1 h at 37 °C, 5% CO_2, and 95% humidity. The same conditions were replicated with the addition of 5 μg/mL of anti-CD47. Excess peptide was washed with PBS, and then macrophages were fixed. Permeabilization of the macrophages was achieved with 0.5% Triton-X for 30 min. After washing with PBS, the macrophages were incubated with 1:100 mouse anti-pTyr (Santa Cruz Biotechnology) for 1 h at RT with gentle shaking. Macrophages were washed with PBS, stained with AlexaFluor 488 donkey anti-mouse (1:1000; Invitrogen) and 1 μg/mL Hoechst 33342 for 1 h with shaking, and then washed again. Fluorescence imaging and quantification were performed as described above.

Intravenous Injections of nS-FF into Mice.

The 14-week-old C57BL6/J mice (Jackson Laboratory, Inc.) were anesthetized with 4% isoflurane in air carrier gas, and approximately 140 μL of blood was drawn retro-orbitally at days −7, −1, and +4 post-injection of either 100 μL of PBS (vehicle control) or 1 mg/kg of ns-FF peptide in 100 μL of PBS. Blood was collected with capillary tubes pre-rinsed with 0.5M EDTA into K_2EDTA microhematocrit tubes to prevent clotting. Injections were given intravenously daily on days 0, 1, 2, and 3. Mice were weighed at each blood draw.

GEO Microarray Analysis.

Data from the GEO database were used to obtain gene expression data for key genes associated with macrophage identity. The cell types included in this analysis were human HEK 293T (GEO accession GSE28715), human PMA-differentiated THP-1 macrophages (GEO accession GDS4258), primary mouse macrophages (GEO accession GDS2454), and human K562 erythroleukemia (GEO accession GSE16774 and GSE8832).

Flow Cytometry.

Fresh human RBCs were washed twice with 50 mM EDTA and then twice with 5% w/v bovine serum albumin (BSA; Sigma) in PBS. K562 cells were collected and washed twice with 5% BSA. RBCs and K562 cells were blocked with 5% BSA for 1 h at RT on a rotator. Saturating amounts of AlexaFluor 647 mouse anti-human CD47 (B6H12; BD Biosciences) were added to both RBCs and K562 cells and incubated at RT on a rotator for 1 h. Cells were washed three times with 5% BSA. Flow cytometry was performed on a BD LSRII (Benton Dickinson) at the Penn Cytomics and Cell Sorting Resources Laboratory and analyzed with FCS Express 7 software (De Novo Software).

Supplementary Material

Refer to Web version on PubMed Central for supplementary material.

ACKNOWLEDGMENTS

We thank the Chenoweth laboratory for helpful discussions, the Cell and Developmental Biology Microscopy Core, and the Penn Cytomics and Cell Sorting Resources Laboratory for facilities. A.R.J. was supported under the National Science Foundation Materials Science and Engineering Center award DMR-1120901, National Heart Lung and Blood Institute grant R01-HL124106-06, and National Cancer Institute grant U54 CA193417. B.H.H. and J.C.A. were supported under DGE-1845298 by the National Science Foundation Graduate Research Fellowship Program.

REFERENCES

(1). Veillette A; Thibaudeau E; Latour SHigh Expression of Inhibitory Receptor SHPS-1 and Its Association with Protein-Tyrosine Phosphatase SHP-1 in Macrophages. J. Biol. Chem1998, 273, 22719–22728. [PubMed: 9712903]

(2). Barclay ANSignal Regulatory Protein Alpha (SIRPα)/Cd47 Interaction and Function. Curr. Opin. Immunol2009, 21, 47–52. [PubMed: 19223164]

(3). Hatherley D; Harlos K; Dunlop DC; Stuart DI; Barclay ANThe Structure of the Macrophage Signal Regulatory Protein Alpha (SIRPα) Inhibitory Receptor Reveals a Binding Face Reminiscent of That Used by T Cell Receptors. J. Biol. Chem2007, 282, 14567–14575. [PubMed: 17369261]

(4). Hatherley D; Graham SC; Turner J; Harlos K; Stuart DI; Barclay ANPaired Receptor Specificity Explained by Structures of Signal Regulatory Proteins Alone and Complexed with CD47. Mol. Cell2008, 31, 266–277. [PubMed: 18657508]

(5). Sharma P; Allison JPImmune Checkpoint Targeting in Cancer Therapy: Toward Combination Strategies with Curative Potential. Cell2015, 161, 205–214. [PubMed: 25860605]

(6). Sharma P; Allison JPThe Future of Immune Checkpoint Therapy. Science2015, 348, 56–61. [PubMed: 25838373]

(7). Yang JC; Hughes M; Kammula U; Royal R; Sherry RM; Topalian SL; Suri KB; Levy C; Allen T; Mavroukakis S; Lowy I; White DE; Rosenberg SAIpilimumab (Anti-CTLA4 Antibody) Causes

Regression of Metastatic Renal Cell Cancer Associated with Enteritis and Hypophysitis. J. Immunother2007, 30, 825. [PubMed: 18049334]

(8). van den Eertwegh AJM; Versluis J; van den Berg HP; Santegoets SJAM; van Moorselaar RJA; van der Sluis TM; Gall HE; Harding TC; Jooss K; Lowy I; Pinedo HM; Scheper RJ; Stam AGM; von Blomberg BME; de Gruijl TD; Hege K; Sacks N; Gerritsen WRCombined Immunotherapy with Granulocyte-Macrophage Colony-Stimulating Factor-Transduced Allogeneic Prostate Cancer Cells and Ipilimumab in Patients with Metastatic Castration-Resistant Prostate Cancer: A Phase 1 Dose-Escalation Trial. Lancet Oncol. 2012, 13, 509–517. [PubMed: 22326922]

(9). Hodi FS; O'Day SJ; McDermott DF; Weber RW; Sosman JA; Haanen JB; Gonzalez R; Robert C; Schadendorf D; Hassel JC; Akerley W; van den Eertwegh AJM; Lutzky J; Lorigan P; Vaubel JM; Linette GP; Hogg D; Ottensmeier CH; Lebbe C; Peschel C; et al. Improved Survival with Ipilimumab in Patients with Metastatic Melanoma. N. Engl. J. Med2010, 363, 711–723. [PubMed: 20525992]

(10). Brahmer JR; Tykodi SS; Chow LQM; Hwu W; Topalian SL; Hwu P; Drake CG; Camacho LH; Kauh J; Odunsi K; Pitot HC; Hamid O; Bhatia S; Martins R; Eaton K; Chen S; Salay TM; Alaparthy S; Grosso JF; Korman AJ; et al. Safety and Activity of Anti-PD-L1 Antibody in Patients with Advanced Cancer. N. Engl. J. Med2012, 366, 2455–2465. [PubMed: 22658128]

(11). Ansell SM; Lesokhin AM; Borrello I; Halwani A; Scott EC; Gutierrez M; Schuster SJ; Millenson MM; Cattry D; Freeman GJ; Rodig SJ; Chapuy B; Ligon AH; Zhu L; Grosso JF; Kim SY; Timmerman JM; Shipp MA; Armand PPD-1 Blockade with Nivolumab in Relapsed or Refractory Hodgkin's Lymphoma. N. Engl. J. Med2015, 372, 311–319. [PubMed: 25482239]

(12). Rodriguez PL; Harada T; Christian DA; Pantano DA; Tsai RK; Discher DEMinimal "Self" Peptides That Inhibit Phagocytic Clearance and Enhance Delivery of Nanoparticles. Science2013, 339, 971–975. [PubMed: 23430657]

(13). Fujioka Y; Matozaki T; Noguchi T; Iwamatsu A; Yamao T; Takahashi N; Tsuda M; Takada T; Kasuga MA Novel Membrane Glycoprotein, SHPS-1, That Binds the SH2-Domain-Containing Protein Tyrosine Phosphatase SHP-2 in Response to Mitogens and Cell Adhesion. Mol. Cell. Biol1996, 16, 6887–6899. [PubMed: 8943344]

(14). Oldenborg P; Gresham H; Lindberg FCD47-Signal Regulatory Protein Alpha (SIRPα) Regulates Fc Gamma and Complement Receptor-Mediated Phagocytosis. J. Exp. Med2001, 193, 855–861. [PubMed: 11283158]

(15). Tsai RK; Discher DEInhibition of "Self" Engulfment through Deactivation of Myosin-II at the Phagocytic Synapse between Human Cells. J. Cell Biol2008, 180, 989–1003. [PubMed: 18332220]

(16). Ishikawa-Sekigami T; Kaneko Y; Okazawa H; Tomizawa T; Okajo J; Saito Y; Okuzawa C; Sugawara-Yokoo M; Nishiyama L; Ohnishi H; Matozaki T; Nojima YSHPS-1 Promotes the Survival of Circulating Erythrocytes through Inhibition of Phagocytosis by Splenic Macrophages. Blood2006, 107, 341–348. [PubMed: 16141346]

(17). Kant A; De P; Peng X; Yi T; Rawlings D; Kim J; Durden DSHP-1 Regulates Fc Gamma Receptor-Mediated Phagocytosis and the Activation of RAC. Blood2002, 100, 1852–1859. [PubMed: 12176909]

(18). Johansen ML; Brown EJDual Regulation of SIRP Alpha Phosphorylation by Integrins and CD47. J. Biol. Chem2007, 282, 24219–24230. [PubMed: 17584740]

(19). Sikic BI; Lakhani N; Patnaik A; Shah SA; Chandana SR; Rasco D; Colevas AD; O'Rourke T; Narayanan S; Papadopoulos K; Fisher GA; Villalobos V; Prohaska SS; Howard M; Beeram M; Chao MP; Agoram B; Chen JY; Huang J; Axt M; et al. First-in-Human, First-in-Class Phase I Trial of the Anti-CD47 Antibody Hu5F9-G4 in Patients with Advanced Cancers. J. Clin. Oncol2019, 37, 946–953. [PubMed: 30811285]

(20). Weiskopf K; Ring AM; Ho CCM; Volkmer J; Levin AM; Volkmer AK; Ozkan E; Fernhoff NB; van de Rijn M; Weissman IL; Garcia KCEngineered SIRP Alpha Variants as Immunotherapeutic Adjuvants to Anticancer Antibodies. Science2013, 341, 88–91. [PubMed: 23722425]

(21). A Trial of TTI-621 for Patients with Hematologic Malignancies and Selected Solid Tumors; Trillium Therapeutics Inc.: Mississauga, Canada.

(22). A Trial of TTI-622 in Patients with Advanced Relapsed or Refractory Lymphoma or Myeloma (TTI-622-01); Trillium Therapeutics Inc.: Mississauga, Canada.

(23). Kauder SE; Kuo TC; Chen A; Harrabi O; Rocha SS; Doyle L; Bollini S; Han B; Sangalang ERB; Sim J; Randolph S; Pons J; Wan HIALX148 Is a High Affinity Sirpa Fusion Protein That Blocks CD47, Enhances the Activity of Anti-Cancer Antibodies and Checkpoint Inhibitors, and Has a Favorable Safety Profile in Preclinical Models. Blood2017, 130, 112–112.

(24). Advani R; Flinn I; Popplewell L; Forero A; Bartlett NL; Ghosh N; Kline J; Roschewski M; LaCasce A; Collins GP; Tran T; Lynn J; Chen JY; Volkmer J; Agoram B; Huang J; Majeti R; Weissman IL; Takimoto CH; Chao MP; Smith SMCD47 Blockade by Hu5F9-G4 and Rituximab in Non-Hodgkin's Lymphoma. N. Engl. J. Med2018, 379, 1711–1721. [PubMed: 30380386]

(25). Alvey C; Discher DEEngineering Macrophages to Eat Cancer: from "Marker of Self" CD47 and Phagocytosis to Differentiation. J. Leukocyte Biol2017, 102, 31–40. [PubMed: 28522599]

(26). Andrechak JC; Dooling LJ; Discher DEThe Macrophage Checkpoint CD47: SIRP Alpha for Recognition of 'Self' Cells: from Clinical Trials of Blocking Antibodies to Mechanobiological Fundamentals. Philos. Trans. R. Soc., B2019, 374, 20180217.

(27). Huang Y; Ma Y; Gao P; Yao ZTargeting CD47: The Achievements and Concerns of Current Studies on Cancer Immunotherapy. J. Thorac. Dis2017, 9, E168–E174. [PubMed: 28275508]

(28). Jalil AR; Andrechak JC; Discher DEMacrophage Checkpoint Blockade: Results from Initial Clinical Trials, Binding Analyses, and CD47-SIRPa Structure-Function. Antibody Ther2020, 3, 80–94.

(29). Lee WY; Weber DA; Laur O; Stowell SR; Mccall I; Andargachew R; Cummings RD; Parkos CAThe Role of Cis Dimerization of Signal Regulatory Protein Alpha (SIRP Alpha) in Binding to CD47. J. Biol. Chem2010, 285, 37953–37963. [PubMed: 20826801]

(30). Oesterhelt F; Rief M; Gaub HESingle Molecule Force Spectroscopy by AFM Indicates Helical Structure of Poly(ethylene-Glycol) in Water. New J. Phys1999, 1, 6.

(31). Hayes BH; Tsai RK; Dooling LJ; Kadu S; Lee JY; Pantano D; Rodriguez PL; Subramanian S; Shin J; Discher DEMacrophages Eat More after Disruption of Cis Interactions between CD47 and the Checkpoint Receptor SIRPa. J. Cell Sci2020, 133, jcs237800. [PubMed: 31964705]

(32). Posner B; Khan M; Bergeron JEndocytosis of Peptide-Hormones and Other Ligands. Endocr. Rev1982, 3, 280–298. [PubMed: 6126355]

(33). Puthenveedu MA; Lauffer B; Temkin P; Vistein R; Carlton P; Thorn K; Taunton J; Weiner OD; Parton RG; von Zastrow MSequence-Dependent Sorting of Recycling Proteins by Actin-Stabilized Endosomal Microdomains. Cell2010, 143, 761–773. [PubMed: 21111236]

(34). Gordon SPhagocytosis: An Immunobiologic Process. Immunity2016, 44, 463–475. [PubMed: 26982354]

(35). Blanco F; Rivas G; Serrano LA Short Linear Peptide That Folds into a Native Stable Beta-Hairpin in Aqueous-Solution. Nat. Struct. Mol. Biol1994, 1, 584–590.

(36). Viguera A; Jimenez M; Rico M; Serrano LConformational Analysis of Peptides Corresponding to Beta-Hairpins and a Beta-Sheet That Represent the Entire Sequence of the Alpha-Spectrin SH3 Domain. J. Mol. Biol1996, 255, 507–521. [PubMed: 8568894]

(37). Bochicchio B; Pepe A; Crudele M; Belloy N; Baud S; Dauchez MTuning Self-Assembly in Elastin-Derived Peptides. Soft Matter2015, 11, 3385–3395. [PubMed: 25811498]

(38). Petrova PS; Viller NN; Wong M; Pang X; Lin GHY; Dodge K; Chai V; Chen H; Lee V; House V; Vigo NT; Jin D; Mutukura T; Charbonneau M; Truong T; Viau S; Johnson LD; Linderoth E; Sievers EL; Vareki SM; et al. TTI-621 (SIRP Alpha Fc): A CD47-Blocking Innate Immune Checkpoint Inhibitor with Broad Antitumor Activity and Minimal Erythrocyte Binding. Clin. Cancer Res2017, 23, 1068–1079. [PubMed: 27856600]

(39). Sun LPeptide-Based Drug Development Advantages and Disadvantages. Mod. Chem. Appl2013, 1, 1–2.

(40). Pytela R; Pierschbacher MD; Argraves S; Suzuki S; Ruoslahti EArginine-Glycine-Aspartic Acid Adhesion Receptors. Methods Enzymol. 1987, 144, 475–489. [PubMed: 2442581]

(41). Schense J; Hubbell JThree-Dimensional Migration of Neurites Is Mediated by Adhesion Site Density and Affinity. J. Biol. Chem2000, 275, 6813–6818. [PubMed: 10702239]

(42). Reardon DA; Fink KL; Mikkelsen T; Cloughesy TF; O'Neill A; Plotkin S; Glantz M; Ravin P; Raizer JJ; Rich KM; Schiff D; Shapiro WR; Burdette-Radoux S; Dropcho EJ; Wittemer SM; Nippgen J; Picard M; Nabors LBRandomized Phase II Study of Cilengitide, an Integrin-

Targeting Arginine-Glycine-Aspartic Acid Peptide, in Recurrent Glioblastoma Multiforme. J. Clin. Oncol2008, 26, 5610–5617. [PubMed: 18981465]

(43). Chames P; Van Regenmortel M; Weiss E; Baty DTherapeutic Antibodies: Successes, Limitations and Hopes for the Future. Br. J. Pharmacol2009, 157, 220–233. [PubMed: 19459844]

(44). Verma V; Sprave T; Haque W; Simone CB; Chang JY; Welsh JW; Thomas CRA Systematic Review of the Cost and Cost-Effectiveness Studies of Immune Checkpoint Inhibitors. Journal for ImmunoTherapy of Cancer2018, 6, 1–15. [PubMed: 29298730]

(45). Hernandez I; Bott SW; Patel AS; Wolf CG; Hospodar AR; Sampathkumar S; Shrank WHPricing of Monoclonal Antibody Therapies: Higher if Used for Cancer?Am. J. Manag. Care2018, 24, 109–112. [PubMed: 29461857]

(46). Hatherley D; Lea SM; Johnson S; Barclay ANPolymorphisms in the Human Inhibitory Signal-Regulatory Protein Alpha Do Not Affect Binding to Its Ligand CD47. J. Biol. Chem2014, 289, 10024–10028. [PubMed: 24550402]

(47). Lin Y; Yan X; Yang F; Yang X; Jiang X; Zhao X; Zhu B; Liu L; Qin H; Liang Y; Han HSoluble Extracellular Domains of Human SIRP Alpha and CD47 Expressed in Escherichia Coli Enhances the Phagocytosis of Leukemia Cells by Macrophages *in Vitro*. Protein Expression Purif. 2012, 85, 109–116.

(48). Ho CCM; Guo N; Sockolosky JT; Ring AM; Weiskopf K; Ozkan E; Mori Y; Weissman IL; Garcia KC"Velcro" Engineering of High Affinity CD47 Ectodomain as Signal Regulatory Protein Alpha (SIRP Alpha) Antagonists That Enhance Antibody-Dependent Cellular Phagocytosis. J. Biol. Chem2015, 290, 12650–12663. [PubMed: 25837251]

(49). Chowdhury S; Castro S; Coker C; Hinchliffe TE; Arpaia N; Danino TProgrammable Bacteria Induce Durable Tumor Regression and Systemic Antitumor Immunity. Nat. Med2019, 25, 1057–1063. [PubMed: 31270504]

(50). Shields CW; Evans MA; Wang LL; Baugh N; Iyer S; Wu D; Zhao Z; Pusuluri A; Ukidve A; Pan DC; Mitragotri SCellular Backpacks for Macrophage Immunotherapy. Science Advances2020, 6, No. eaaz6579. [PubMed: 32494680]

(51). Cox D; Greenberg SPhagocytic Signaling Strategies: Fc(gamma) Receptor-Mediated Phagocytosis as a Model System. Semin. Immunol2001, 13, 339–345. [PubMed: 11708889]

(52). Bakalar MH; Joffe AM; Schmid EM; Son S; Podolski M; Fletcher DASize-Dependent Segregation Controls Macrophage Phagocytosis of Antibody-Opsonized Targets. Cell2018, 174, 131. [PubMed: 29958103]

(53). Sockolosky JT; Dougan M; Ingram JR; Ho CCM; Kauke MJ; Almo SC; Ploegh HL; Garcia KCDurable Antitumor Responses to CD47 Blockade Require Adaptive Immune Stimulation. Proc. Natl. Acad. Sci. U. S. A2016, 113, E2646–E2654. [PubMed: 27091975]

(54). Stahl PJ; Cruz JC; Li Y; Yu SM; Hristova KOn-the-Resin N-Terminal Modification of Long Synthetic Peptides. Anal. Biochem2012, 424, 137–139. [PubMed: 22387389]

(55). Anthis NJ; Clore GMSequence-Specific Determination of Protein and Peptide Concentrations by Absorbance at 205 nm. Protein Science2013, 22, 851–858. [PubMed: 23526461]

(56). Goldfarb A; Saidel L; Mosovich EThe Ultraviolet Absorption Spectra of Proteins. J. Biol. Chem1951, 193, 397–404. [PubMed: 14907727]

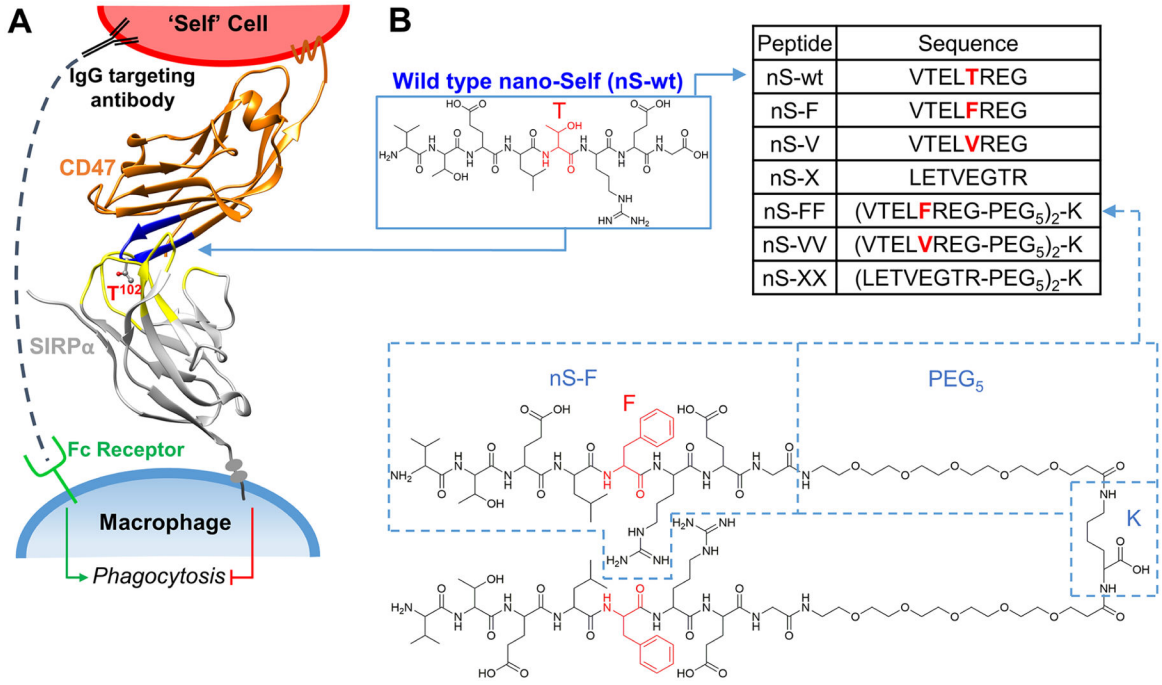

Peptide	Sequence
nS-wt	VTELTREG
nS-F	VTELFREG
nS-V	VTELVREG
nS-X	LETVEGTR
nS-FF	(VTELFREG-PEG$_5$)$_2$-K
nS-VV	(VTELVREG-PEG$_5$)$_2$-K
nS-XX	(LETVEGTR-PEG$_5$)$_2$-K

Figure 1.

nano-Self peptides are designed as competitive inhibitors based on CD47's key binding loop. (A) "Marker of Self" CD47 is expressed on all cells and inhibits phagocytosis of "Self" cells when it binds its receptor SIRPα on macrophages (Protein Database accession number: 2JJS). (B) The nS-wt peptide consists of eight amino acids (blue) that bind the SIRPα binding pocket (yellow). Substitutions of the Thr residue (red) generate nS peptides as competitive antagonists against SIRPα. nS-X is a scrambled sequence. Bivalent peptides were constructed by linking monomers to (di-PEG)-lysine *via* their C-termini.

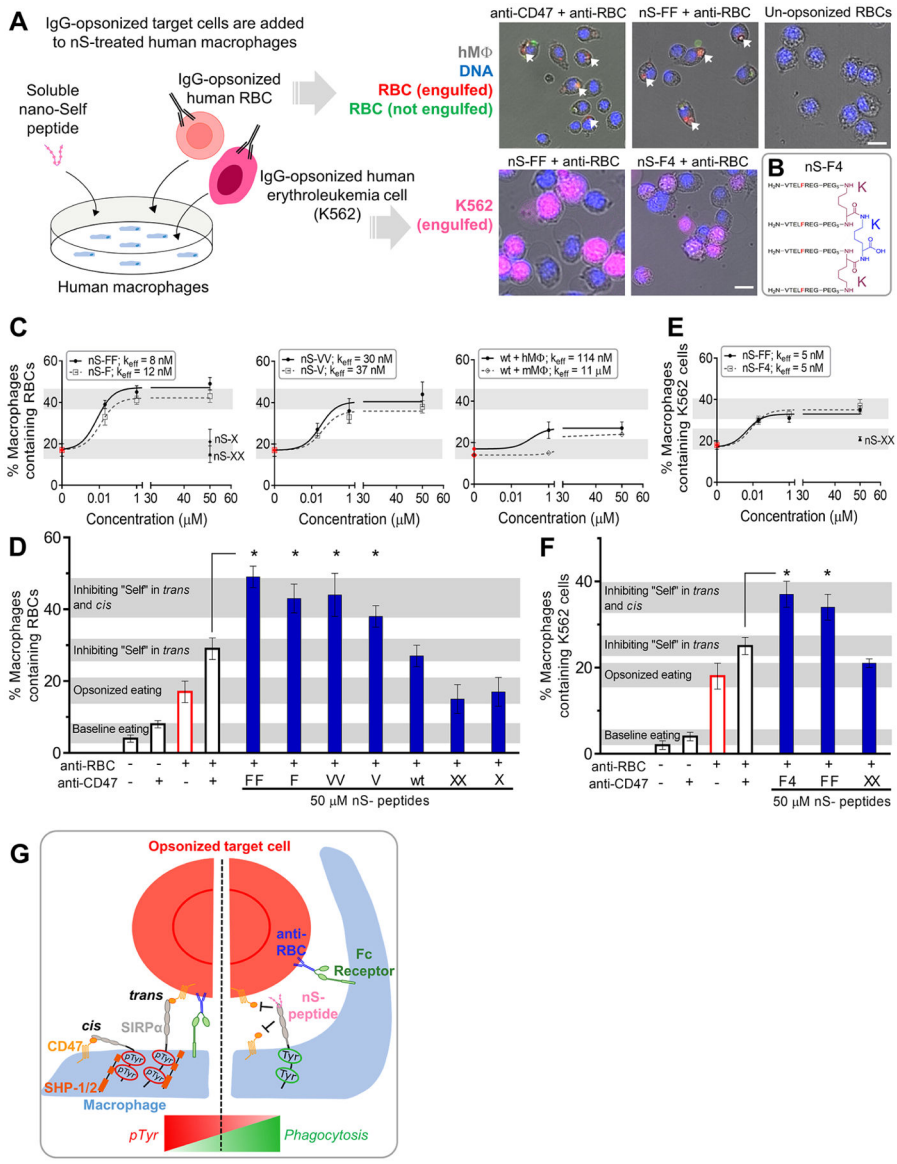

Figure 2.

Multivalent nano-Self peptides enhance human macrophage phagocytosis of IgG opsonized targets. (A) Schematic of the phagocytosis assay. RBC and K562 erythroleukemia cell opsonization by anti-human IgG is followed by addition of the cell suspensions to cultured macrophages togther with the soluble nS peptides. Phagocytosis is measured by counting macrophages with internalized, fluorescent target cells (scale bar: 25 μm). (B) Sketch of the tetravalent nS-F4 which consists of a core lysine (blue K) coupled via two lysines (red K's) with four amines coupled to nS-F's. (C) Incubating various concentrations of nS peptides with macrophages results in varying levels of macrophages that internalize at least one IgG-opsonized RBC. Relative to nS-wt, suitable substitutions of the key Thr enhanced phagocytosis as did multivalency. Scrambled nS-X or nS-XX peptides do not affect phagocytosis with IgG alone (red points). Phagocytosis by mouse macrophages is also affected by nS-wt, albeit not as much as with human macrophages. At least

200 macrophages were analyzed per condition (hMφ: human macrophages; mMφ: mouse macrophages; $n = 3 \pm$ SEM). (D) Saturating macrophages with nS-FF, nS-F, and nS-VV enhances phagocytosis by an additional ~10–20% relative to anti-CD47 treatment of opsonized RBCs. nS-wt is least effective but gives the same result as anti-CD47 and exceeds opsonization alone ($n = 3 \pm$ SEM; * denotes $p < 0.05$ relative to CD47-blocked and opsonized RBCs). (E) Phagocytosis of IgG-opsonized K562 erythroleukemia cells is enhanced by nS-FF and nS-F4. (F) Saturating macrophages with nS-FF and nS-F4 increases phagocytosis of opsonized K562 cancer cells relative to opsonized and CD47 blocked cells, but nS-XX has no effect on IgG-driven engulfment. (G) Schematic of how nS peptides engage and enhance phagocytosis. Left panel: CD47-expressing cells signal “self” through *trans* engagement with SIRPα on the macrophage, increasing pTyr signals, and overriding prophagocytic signaling from the opsonizing IgG. Right panel: nS peptides in solution engage with SIRPα, inhibiting *trans* binding of CD47 on opsonized cells and also inhibiting *cis* binding on the macrophages, leading to increased phagocytosis.

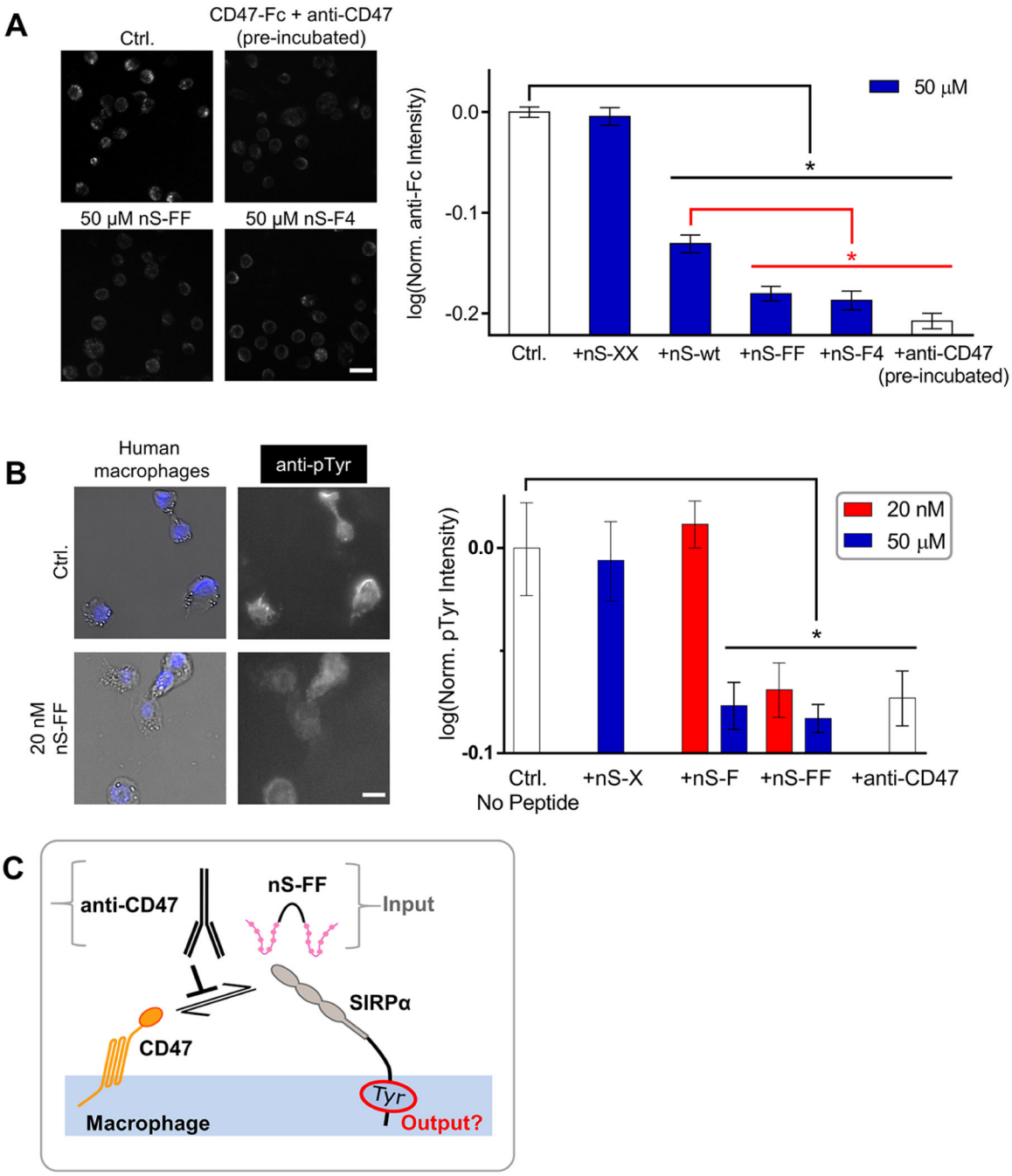

Figure 3.

Interactions of nano-Self peptides with macrophages are consistent with SIRPα binding, blocking, and signaling. (A) Representative fluorescence microscopy images of CD47-Fc binding to macrophages as visualized with fluorescent anti-Fc (Ctrl) and also inhibited by nS-wt, nS-FF and nS-F4 peptides but not by scrambled nS-XX. Anti-CD47 and CD47-Fc were incubated together prior to their addition to macrophages. All conditions compared to saturating concentration of CD47-Fc (n = 2 sets of triplicates, mean ± SEM; * denotes $p < 0.05$; scale bar: 50 μm). (B) Basal levels of pTyr signal are observed in isolated

macrophages. The pTyr signal is suppressed by nS-FF even at nM concentration, whereas monovalent nS-F requires μM concentration. This inhibition of phosphorylation is not observed with nS-X ($n = 3 \pm$ SEM; * denotes $p < 0.05$ relative to control; scale bar: 25 μm). (C) Schematic of nS peptides and anti-CD47 antagonizing the *cis* macrophage checkpoint and thereby suppressing pTyr.

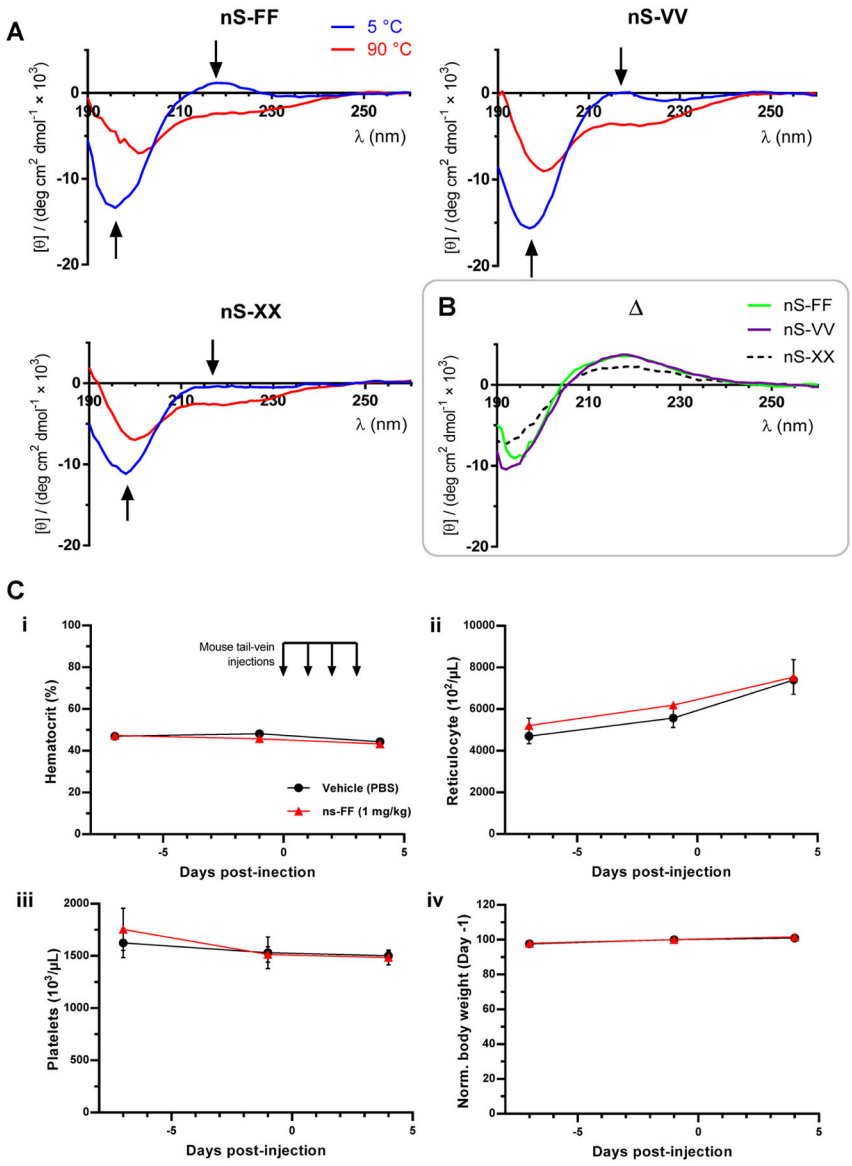

Figure 4.

Solution structure and *in vivo* safety data. (A) Random coil structure with low hairpin content suggests an induced fit mechanism into the SIRPα binding pocket. CD spectra of nS-FF, nS-VV, nS-XX at 5 and 90 °C. Arrows indicate the molar ellipticity at 215–220 and 195 nm, respectively, suggestive of a β-hairpin turn which is lost in nS-XX. (B) Difference plots show that nS-FF and nS-VV agree in terms of structure, consistent with phagocytosis results. (C) Phase-1 type pre-clinical trial of lead peptide, nS-FF: Intravenous injections of nS-FF were done for four consecutive days followed by blood withdrawal 24 h after last injection. Blood parameters show that nS-FF at 1 mg/kg is safe, with no anemia or weight loss.